

Second-harmonic generation as probe for structural and electronic properties of buried GaP/Si(001) interfaces

K. Brixius,¹ A. Beyer,¹ G. Mette,¹ J. Gdde,¹ M. Drr,² W. Stolz,¹ K. Volz,¹ and U. Hfer^{1, *}

¹*Fachbereich Physik und Zentrum fr Materialwissenschaften,
Philipps-Universitt, D-35032 Marburg, Germany*

²*Institut fr Angewandte Physik, Justus-Liebig-Universitt Gießen, D-35392 Gießen, Germany*

(Dated: November 1, 2018)

Optical second-harmonic generation (SHG) is demonstrated to be a sensitive probe of the buried interface between the lattice-matched semiconductors gallium phosphide and silicon with (001) orientation. *Ex situ* rotational anisotropy measurements on GaP/Si heterostructures show a strong isotropic component of the second-harmonic response not present for pure Si(001) or GaP(001). The strength of the overlying anisotropic response directly correlates with the quality of the interface as determined by atomically resolved scanning transmission electron microscopy. Systematic comparison of samples fabricated under different growth conditions in metal-organic vapor phase epitaxy reveals that the anisotropy for different polarization combinations can be used as a selective fingerprint for the occurrence of anti-phase domains and twins. This all-optical technique can be applied as an *in situ* and non-invasive monitor even during growth.

The investigation of interfacial properties is one of the most challenging tasks in modern material science and engineering of electronic devices. Within the last few years large efforts have been made on the structural analysis of interfaces by means of cross-sectional scanning tunneling microscopy, atomic force microscopy or scanning transmission electron microscopy (STEM). The latter technique is particularly suited for this purpose because it can yield element specific information about interfaces of inorganic materials with atomic resolution [1, 2]. However, all these methods require a preceding invasive preparation of the samples in order to access the respective interface in *ex situ* experiments.

In contrast to these methods, all-optical techniques allow a non-invasive *in situ* access to interfaces, which is basically only limited by the optical absorption length of the investigated material system. Moreover, even-order nonlinear optical techniques such as second-harmonic generation (SHG) intrinsically have a high interface sensitivity owing to the symmetry breaking at the crystal surface and at interfaces [3–5]. The interface sensitivity is particularly high for centrosymmetric materials where the bulk second-order susceptibility $\chi^{(2)}$ vanishes in dipole approximation. However, even in non-centrosymmetric polar materials with strong nonlinear bulk response such as GaAs or GaP, high interface sensitivity can be achieved by suppressing the bulk response for specific polarization combinations of the incoming fundamental and generated second-harmonic (SH) light [6, 7].

Here, we combine STEM and SHG to investigate the interface between the III/V-material gallium phosphide and silicon which represents a model system for the growth of a polar on a nonpolar semiconductor and which promises many application for optoelectronic applications based on silicon electronics [8–13]. This system

is of particular interest because the lattice mismatch between GaP(001) and Si(001) is small. Therefore, strain induced defects can be neglected. Nevertheless, the heteroepitaxial growth is challenging because the interface is not automatically charge neutral and anti-phase domains (APDs) can be formed at monoatomic steps of the substrate [14, 15]. Moreover, stacking faults and twins can be formed in the GaP film. The latter occur if a part of the crystal is rotated with respect to the main crystal orientation. The structure of these defects has been extensively investigated by means of STEM [16–18]. In order to optimize the conditions for a defect-free growth, however, an *in situ* technique for the evaluation of the interface quality during growth would represent a great progress towards an detailed understanding of the interface formation and for the preparation of highly efficient devices.

Here, we show that SHG is able to non-invasively investigate the properties of the buried interface between GaP and Si and that it is possible to directly relate the SHG anisotropy to the interface quality. For this purpose we have prepared GaP/Si samples by metal-organic vapor phase epitaxy (MOVPE) under different growth conditions that give rise to specific defects such as APDs or twins. We present sets of the rotational anisotropy of the second-harmonic intensity for different polarization combinations of the incoming fundamental and generated second harmonic in reflection and compare these results with atomically resolved STEM measurements. The combination of both experimental techniques allows us to identify the occurrence of specific defects in the second-harmonic anisotropy for particular polarization combinations. This makes it feasible to use second-harmonic anisotropy as an *in situ*, non-invasive probe for the interface quality even during growth. It would be complementary to other optical techniques like reflection anisotropy spectroscopy which is particularly used to monitor the surface properties under growth conditions in a MOVPE reactor [19].

*hoefer@physik.uni-marburg.de

The experiments were performed under ambient conditions using 50-fs laser pulses generated by a femtosecond Ti:Sapphire laser amplifier system operating at 800 nm at a repetition rate of 15 kHz. The linear polarized laser beam at fundamental frequency ω was focussed under an angle of 45° onto the sample as illustrated in Fig.1 (a). The generated second-harmonic light at frequency 2ω was observed in reflection for a chosen combination of input and output polarization, e.g. p -polarized incident light and s -polarized 2ω -light (abbreviated by pS). Standard boxcar-integrator technique was used for detection as described in detail in Ref. 20. The SH signal has been normalized with respect to a reference that was generated in a quartz crystal in pP configuration. The rotational anisotropy of the SH intensity was measured by rotating the sample around the surface normal (z -axis) as characterized by the azimuthal angle Ψ . The samples were oriented such that for $\Psi = 0^\circ$ (180°) the $[\bar{1}10]$ - ($[1\bar{1}0]$)-direction was lying within the plane of incidence (cf. Fig.1 (a)). The fluence of the incident laser radiation was kept at least one order of magnitude below 100 mJ/cm^2 which we determined as the threshold for multishot damage of our samples.

The investigated GaP/Si heterostructures were grown by metal-organic vapor phase epitaxy (MOVPE) in an Aixtron AIX 200 GFR reactor using triethylgallium (TEGa) and tertiary-butyl phosphine (TBP) as precursors for gallium and phosphorus, respectively. Four samples were prepared by using flow-rate modulated epitaxy (FME), for which TEGa and the TBP were supplied intermittently in a total of sixteen cycles, starting with TEGa. The supply of GaP per cycle was varied between 0.2 to 1.36 monolayer by a variation of the partial pressure of TEGa between 7.6×10^{-4} and 7.6×10^{-3} mbar while holding the TBP pressure constant at 0.91 mbar. In the following, these samples are referred to as FME0.20ML and so forth. For one sample, the continuous growth mode (CGM) was used, in which TEGa and TBP were applied simultaneously. The total thickness of the layers varied between 0.8 and 4.5 nm as determined by X-ray reflection in an X'Pert Pro diffractometer. The structural characterization of the GaP/Si interfaces was carried out in a JEOL 2200FS scanning transmission electron microscope operating at 200 kV. This STEM can achieve atomic resolution in the high-angle annular dark-field imaging mode by aberration corrections of the probe forming lenses. For comparison, we also studied the SH response of the individual materials. In case of Si, a native oxide covered Si(001) wafer was used. In case of GaP, a $1 \mu\text{m}$ thick GaP film was grown epitaxially on a GaP(001) wafer.

The azimuthal dependence of the SH intensity for all samples and polarization combinations is presented in Fig. 1 (b)-(h). These rotation patterns offer a direct access to the symmetry and rotational anisotropy of the second-order nonlinear response [3]. For the GaP wafer (Fig. 1 (g)), a four-fold anisotropy was found for the polarization combinations pP , pS and sP in consistence

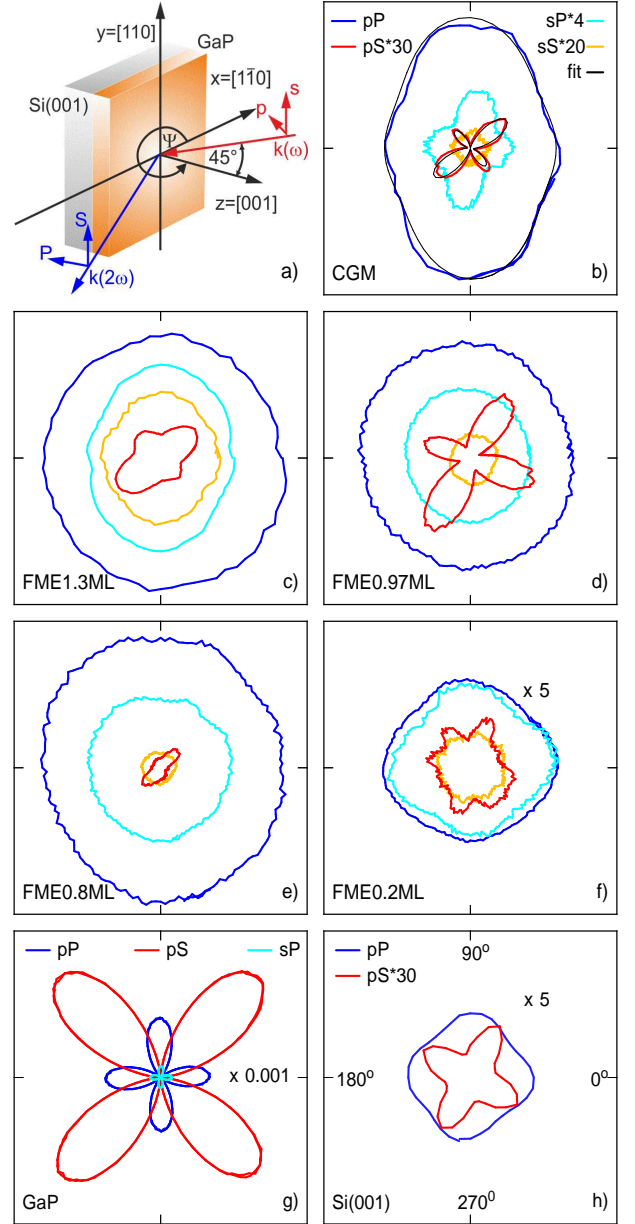


FIG. 1: (Color online) (a) Experimental setup. (b)-(f) Polar plots of the rotational SH anisotropy from five different GaP/Si(001) samples for different polarization combinations of the incoming fundamental and the detected SH as denoted in (b). For comparison, (g) and (h) show the signal of a GaP(001) wafer and a Si(001) wafer, respectively. The signals of the different polarization combinations have been scaled as denoted in the differently figures for better comparison. Black lines in (a) exemplarily show fits of Eq. 1 for the polarization combinations pP and pS .

with other reports [6]. This anisotropy results from the $43m$ -symmetry group of zincblende crystals and is a pure bulk dipole contribution. The pS -combination shows the strongest SHG; it vanishes completely if the polarization of the fundamental is along the $[110]$ - and $[\bar{1}10]$ -direction.

In contrast to the GaP wafer, the SH response of the native oxide covered Si(001) wafer (Fig. 1 (h)) is weaker by about four orders of magnitude. Its fourfold anisotropy is known to originate from the bulk quadrupole contribution [21] whereas the isotropic contribution is attributed to the SiO₂ layer or the Si/SiO₂ interface [5]. Within our detection limit, no SH signal could be observed in case of the *sS*-combination for both the GaP and the Si wafer.

Compared to the two individual wafers, the SH response of the five heteroepitaxially grown films of GaP on Si(001) (Fig. 1 (b)-(f)) differs remarkably, both in overall intensity and in particular in anisotropy. Most prominent is the dominant isotropic contribution in the patterns for the *pP* (blue lines) and the *sP* (cyan lines) polarization combination. Except for the thinnest sample FME0.2ML, this signal is considerably larger than the response of the Si wafer. Moreover, it by far outreaches the almost invisible four-fold anisotropic bulk contribution of the GaP films on Si. We therefore assign the isotropic signal to the interface between GaP and Si. Since the GaP wafer was grown under similar conditions as the GaP/Si samples but does not show a measurable isotropic signal, we exclude that the GaP surface contributes significantly to the observed isotropic SH component. This interpretation is supported by additional measurements for GaP layers with thicknesses of up to 65 nm (not shown) which showed that the isotropic contribution of the SH response decreases exponentially with the GaP layer thickness.

A second-order nonlinear response of the interface between two semiconductors can arise either from the presence of a static electric field due to the band alignment of both materials [22] or from the modification of the chemical bonds at the interface. For the GaP/Si interface, the latter is related to the hybridized sp³ orbitals that are distorted due to the Ga-Si and P-Si bonds. Similar, although quantitatively stronger effects, have been observed for the clean Si surface, where a comparable symmetry break due to surface reconstruction results in an increase of the SH intensity by a factor of ~ 100 [23]. In our case of the GaP/Si interface, the increase compared to the oxidized Si surface is only a factor of ~ 10 . This weaker effect might be connected to a cancelation due to bond distortions in opposite directions. An electric field at the interface gives rise to the EFISH-effect [24, 25], which also predominantly contributes to the p-polarized component of the SH intensity because it particularly affects the nonlinear response perpendicular to the interface. It has been demonstrated that fields due to depletion layers can exceed the nonlinear bulk response, even in case of strong bulk signals for III-V materials like GaAs [26, 27]. Most probably, both distorted bonds as well as electric fields at the interface contribute to the observed isotropic response.

The *pS* contribution (red lines in Fig.1) of the SH response seems to be less affected by the interface because its shape is similar to the response of the Si and the GaP wafer. Its strength, however, is almost five orders of magnitude smaller as compared to the bulk response

of the GaP wafer. This is surprising because the penetration depth of the fundamental light $\delta_{\text{GaP},800\text{nm}}$ is about 160 μm and the SH intensity increases up to a film thickness of ~ 30 nm before a reduction due to a phase shift between the ω - and 2ω -light sets in. Therefore, the GaP bulk contribution from thin films of a few nm thickness should only be smaller by about one order of magnitude compared to the thick wafer. This strong reduction of the bulk response is most likely being caused by a destructive interference due to the appearance of anti-phase domains because the phase of the SH response originating from P-polar GaP is shifted by about π in comparison to the response of the Ga-polar GaP. This makes SHG very sensitive to APDs as it was demonstrated for thick GaAs films grown on Si(001) [28].

Beyond these general differences between the SH response of the individual wafers and the GaP/Si samples, the different heterostructures show characteristic variations for all measured polarization combinations. In the following we show that these individual differences of the SH response can be related to structural differences that have been obtained by STEM. This makes it possible to use the nonlinear response as a fingerprint of the GaP/Si interfaces.

For this purpose a symmetry analysis has been applied that quantifies the different isotropic and anisotropic contributions to the nonlinear response. Phenomenologically, the second-harmonic intensity $I_{ij}(2\omega)$ in reflection for a given polarization combination ij can be written as a function of the incidence intensity $I_i(\omega)$ as $I_{ij}(2\omega) \propto |\chi_{\text{eff},ij}^{(2)}|^2 I_i^2(\omega)$ where $\chi_{\text{eff},ij}^{(2)}$ is an effective second-order nonlinear susceptibility tensor of third rank that includes all contributions (surface, interface, bulk, EFISH, etc.) to the second-order nonlinear polarization [3] even if the intrinsic material response of the bulk and EFISH contributions might be in the most general case described by higher-order tensors of the nonlinear susceptibility [25, 29]. The dependence of $I_{ij}(2\omega)$ on the azimuthal angle Ψ can then be written as a Fourier expansion up to the fourth order

$$I_{ij}(2\omega) \propto \left| a_{ij} + \sum_{m=1}^4 b_{ij}^{(m)} \cos m\Psi + c_{ij}^{(m)} \sin m\Psi \right|^2, \quad (1)$$

where the isotropic (a_{ij}) and anisotropic coefficients ($b_{ij}^{(m)}$, $c_{ij}^{(m)}$) contain all optical properties, in particular the corresponding components of the nonlinear susceptibility tensors as well as Fresnel coefficients. For (001) oriented samples, odd orders m can be excluded.

Table I lists the expected non-vanishing isotropic and anisotropic coefficients at the different polarization combinations for all considered SHG sources, i.e. Si-surface, -bulk and -EFISH as well as GaP-bulk and -EFISH.

Within this model the azimuthal dependence of the SH intensity can be well described for all polarization combinations by a least-square fit of the coefficients a_{ij} , $c_{ij}^{(2)}$, $b_{ij}^{(2)}$ and $b_{ij}^{(4)}$, i.e. omitting the $c_{ij}^{(4)}$. Two examples

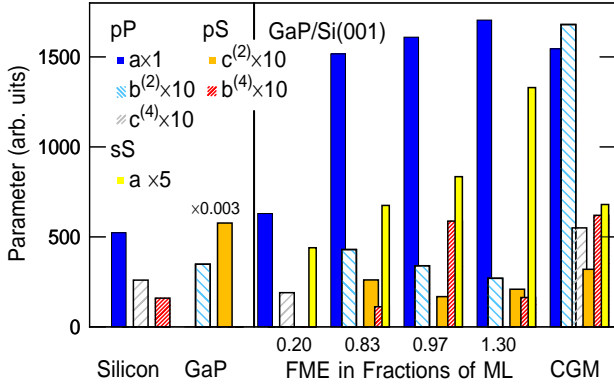


FIG. 2: (Color online) Isotropic and anisotropic coefficients for all investigated samples as obtained by a least-square fit of Eq. 1 for the polarization combinations pP , pS , and sS .

of these fits for the polarization combinations pP and pS are shown in Fig. 1 (b) (black lines).

Figure 2 summarizes the fitting results for the polarization combinations pP , pS , and sS . For all heterostructures, the interface specific isotropic parameter a_{pP} (blue bars) dominates the total response. For the sample with the smallest GaP thickness of 0.8 nm (FME0.20ML), the magnitude of this contribution is comparable to that of the Si wafer. For the other GaP/Si samples including the CGM sample, a_{pP} shows only a small variation. This suggests that the interface properties do not change substantially for GaP layer thicknesses of 1.6 to 4.5 nm.

The STEM images show, however, that the number of defects in the interface-near region of the FEM samples increases considerably for a GaP supply of more than 1 ML per cycle. This is shown exemplary in Fig. 3 (a) and (c) by comparing the STEM images of FEM0.97ML and FEM1.30ML. Whereas the GaP film of sample FEM0.97ML shows no visible defects and a rather abrupt interface, two APDs of opposite polarity can be identified in the left and right part of the STEM image of sample FEM1.30ML. These APDs can form if an excess of TEGa etches Ga droplets into the Si crystal which then serve as nuclei for APDs [30]. The formation of APDs causes an in-plane symmetry reduction that af-

| origin of SHG | pP | pS | sP | sS |
|----------------------------|------------------------|----------------|------------------------|----------------|
| Si surface (single-domain) | $a_{pP}, c_{pP}^{(2)}$ | $b_{pS}^{(2)}$ | $a_{sP}, c_{sP}^{(2)}$ | — |
| Si surface (multi-domain) | a_{pP} | — | a_{sP} | — |
| Si bulk (quadrupole) | $a_{pP}, c_{pP}^{(4)}$ | $b_{pS}^{(4)}$ | $a_{sP}, c_{sP}^{(4)}$ | $b_{sS}^{(4)}$ |
| Si EFISH $\chi^{(3)}$ | a_{pP} | — | a_{sP} | — |
| GaP bulk | $b_{pP}^{(2)}$ | $c_{pS}^{(2)}$ | $b_{sP}^{(2)}$ | — |
| GaP bulk (quadrupole) | $a_{pP}, c_{pP}^{(4)}$ | $b_{pS}^{(4)}$ | $a_{sP}, c_{sP}^{(4)}$ | $b_{sS}^{(4)}$ |
| GaP EFISH $\chi^{(3)}$ | a_{pP} | — | a_{sP} | — |

TABLE I: Isotropic and anisotropic contributions to the SHG from surface, bulk and EFISH of Si(001) and GaP(001) for the different polarization combinations.

fects predominantly the in-plane (s -polarized) SHG components. This is directly reflected by the strong increase of the isotropic a_{sS} contribution (yellow bars in Fig. 2) with increasing TEGa pressure which is characterized by the supply of GaP monolayer per cycle. If APDs grow straight up through the crystal, they typically have a rectangular shape with similar edge lengths in the $[110]$ - and $[\bar{1}10]$ -directions [30]. Such fourfold anisotropy is in fact slightly visible in the sS -component of the rotational SH anisotropy for sample FME1.30ML (yellow line in Fig. 1 (c)).

The STEM measurements on the CGM sample exhibit much less APDs and, consequently, only a small magnitude of a_{sS} is observed in SHG. In this growth mode, however, the formation of twins is favored as discussed in detail in Ref. 16. Such a twin, which is sketched in Fig. 3 (d), can be clearly identified in an STEM image of the CGM sample shown in Fig. 3 (b). It gives rise to a two-fold anisotropy between the $[\bar{1}10]$ and $[110]$ directions because twins predominately form on Ga-terminated $\{111\}A$ planes [16, 31]. This anisotropy is characterized by a large magnitude of $b_{pP}^{(2)}$ (cyan/white bars in Fig. 2) as observed for the CGM sample. In contrast, $b_{pP}^{(2)}$ is comparatively small for all FME samples.

The anisotropy for the pS polarization combination is characterized by the parameters $c_{pS}^{(2)}$ and $b_{pS}^{(4)}$ which are depicted by orange and red/white bars in Fig. 2, respectively. These parameters might be further indicators for the film quality. They show, however, no clear trend for the different growth modes and cannot be correlated to specific defects observed in STEM.

In summary, we have shown that optical second-harmonic generation can be successfully used as a sensitive, non-invasive probe for the quality of the interface between thin films of GaP and Si(001). The rotational anisotropy of the second-harmonic intensity can be correlated to specific defects that form at different growth

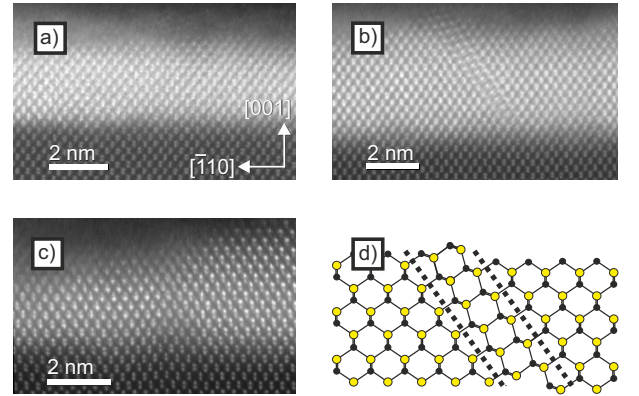


FIG. 3: (Color online) STEM images of the GaP/Si interface for the samples (a) FME0.97ML, (b) CGM, and (c) FME1.30ML. (d) Scheme of twin defect in GaP. Ga and P atoms are depicted by yellow and black dots, respectively.

conditions in metal-organic vapor phase epitaxy. In particular, the occurrence of anti-phase domains and twins are clearly identified. This all-optical technique can be applied as an *in situ* monitor of the growth process com-

plementary to reflection anisotropy spectroscopy.

We gratefully acknowledge funding by the Deutsche Forschungsgemeinschaft through the SFB 1083.

-
- [1] P. M. Voyles, D. A. Muller, J. L. Grazul, P. H. Citrin, and H.-J. L. Gossmann, *Nature* **416**, 826 (2002).
- [2] O. L. Krivanek, M. F. Chisholm, V. Nicolosi, T. J. Pennycook, G. J. Corbin, N. Dellby, M. F. Murfitt, C. S. Own, Z. S. Szilagyi, M. P. Oxley, S. T. Pantelides, and S. J. Pennycook, *Nature* **464**, 571 (2010).
- [3] T. F. Heinz, in *Nonlinear Surface Electromagnetic Phenomena*, edited by H.-E. Ponath and G. I. Stegeman (Elsevier Science Publishers B.V., Amsterdam, 1991), pp. 353–416.
- [4] T. F. Heinz, F. J. Himpsel, E. Palange, and E. Burstein, *Phys. Rev. Lett.* **63**, 644 (1989).
- [5] G. Lupke, *Surf. Sci. Rep.* **35**, 77 (1999).
- [6] T. Stehlin, M. Feller, P. Guyotsionnest, and Y. R. Shen, *Opt. Lett.* **13**, 389 (1988).
- [7] M. S. Yeganeh, J. Qi, A. G. Yodh, and M. C. Tamargo, *Phys. Rev. Lett.* **68**, 3761 (1992).
- [8] S. Liebich, M. Zimprich, A. Beyer, C. Lange, D. J. Franzbach, S. Chatterjee, N. Hossain, S. J. Sweeney, K. Volz, B. Kunert, and W. Stolz, *Appl. Phys. Lett.* **99**, 071109 (2011).
- [9] O. Supplie, M. M. May, G. Steinbach, O. Romanyuk, F. Grosse, A. Nägelein, P. Kleinschmidt, S. Brückner, and T. Hannappel, *J. Phys. Chem. Lett.* **6**, 464 (2015).
- [10] Y. P. Wang, J. Stodolna, M. Bahri, J. Kuyyalil, T. N. Thanh, S. Almosni, R. Bernard, R. Tremblay, M. Da Silva, A. Létoublon, T. Rohel, K. Tavernier, L. Largeau, G. Patriarche, A. Le Corre, A. Ponchet, C. Magen, C. Cornet, and O. Durand, *Appl. Phys. Lett.* **107**, 191603 (2015).
- [11] O. Romanyuk, O. Supplie, T. Susi, M. M. May, and T. Hannappel, *Phys. Rev. B* **94**, 155309 (2016).
- [12] P. Kumar and C. H. Patterson, *Phys. Rev. Lett.* **118**, 237403 (2017).
- [13] I. Lucci, S. Charbonnier, L. Pedesseau, M. Vallet, L. Cerutti, J.-B. Rodriguez, E. Tournié, R. Bernard, A. Létoublon, N. Bertru, A. Le Corre, S. Rennesson, F. Semond, G. Patriarche, L. Largeau, P. Turban, A. Ponchet, and C. Cornet, *Phys. Rev. Materials* **2**, 060401 (2018).
- [14] H. Kroemer, *J. Cryst. Growth* **81**, 193 (1987).
- [15] K. Volz, A. Beyer, W. Witte, J. Ohlmann, I. Nemeth, B. Kunert, and W. Stolz, *J. Cryst. Growth* **315**, 37 (2011).
- [16] A. Beyer, I. Nemeth, S. Liebich, J. Ohlmann, W. Stolz, and K. Volz, *J. Appl. Phys.* **109**, 083529 (2011).
- [17] A. Beyer, B. Haas, K. I. Gries, K. Werner, M. Luysberg, W. Stolz, and K. Volz, *Appl. Phys. Lett.* **103**, 032107 (2013).
- [18] A. Beyer, A. Stegmüller, J. O. Oelerich, J. Kakhaber, K. Werner, G. Mette, W. Stolz, S. D. Baranovskii, R. Tonner, and K. Volz, *Chem. Mater.* **28**, 3265 (2016).
- [19] P. Weightman, D. S. Martin, R. J. Cole, and T. Farrell, *Rep. Prog. Phys.* **68**, 1251 (2005).
- [20] K. Stépán, M. Dürr, J. Güdde, and U. Höfer, *Surf. Sci.* **593**, 54 (2005).
- [21] H. W. K. Tom, T. F. Heinz, and Y. R. Shen, *Phys. Rev. Lett.* **51**, 1983 (1983).
- [22] K. Ishioka, K. Brixius, A. Beyer, A. Rustagi, C. J. Stanton, W. Stolz, K. Volz, U. Höfer, and H. Petek, *Appl. Phys. Lett.* **108**, 051607 (2016).
- [23] U. Höfer, *Appl. Phys. A* **63**, 533 (1996).
- [24] C. H. Lee, R. K. Chang, and N. Bloembergen, *Phys. Rev. Lett.* **18**, 167 (1967).
- [25] O. A. Aktsipetrov, A. A. Fedyanin, J. I. Dadap, and M. C. Downer, *Laser Phys.* **6**, 1142 (1996).
- [26] T. A. Germer, K. W. Kolasinski, J. C. Stephenson, and L. J. Richter, *Phys. Rev. B* **55**, 10694 (1997).
- [27] O. A. Aktsipetrov, A. A. Fedyanin, A. V. Melnikov, E. D. Mishina, A. N. Rubtsov, M. H. Anderson, P. T. Wilson, H. ter Beek, X. F. Hu, J. I. Dadap, and M. C. Downer, *Phys. Rev. B* **60**, 8924 (1999).
- [28] M. Lei, J. Price, W. E. Wang, M. H. Wong, R. Droopad, P. Kirsch, G. Bersuker, and M. C. Downer, *Appl. Phys. Lett.* **102**, 152103 (2013).
- [29] J. E. Sipe, D. J. Moss, and H. M. van Driel, *Phys. Rev. B* **35**, 1129 (1987).
- [30] K. Werner, A. Beyer, J. Oelerich, S. Baranovskii, W. Stolz, and K. Volz, *J. Cryst. Growth* **405**, 102 (2014).
- [31] O. Skibitzki, F. Hatami, Y. Yamamoto, P. Zaumseil, A. Trampert, M. A. Schubert, B. Tillack, W. T. Masselink, and T. Schroeder, *J. Appl. Phys.* **111**, 073515 (2012).